BioImplantable Bone Stress Sensor

J. Fernando Alfaro[1], Lee E. Weiss[1], Phil G. Campbell[3],
Mark C. Miller[4], Christa Heyward[5], John S. Doctor[5] and Gary K. Fedder[1,2]
[1]The Robotics Institute, [2]Department of Electrical and Computer Engineering
[3]Institute for Complex Engineered Systems and Department of Biomedical Engineering
Carnegie Mellon University. Pittsburgh, Pennsylvania 15213
[4]School of Health Sciences and [5]Department of Biological Sciences
Duquesne University. Pittsburgh, Pennsylvania 15282
Email: falfaro@ri.cmu.edu

Abstract— **The clinical management of skeletal trauma and disease relies on radiographic imaging to infer bone quality. However, bone strength does not necessarily correlate well with image intensity. There is a need for a safe and convenient way to measure bone strength *in situ*. This paper presents a new technique to directly measure bone strength *in situ* at a micro-level scale through a MicroElectroMechanical System (MEMS) sensor.**

The proposed MEMS stress sensor comprises an array of piezoresistive sensor "pixels" to detect stress across the interfacial area between the MEMS chip and bone with resolution to 100 Pa, in 1 sec averaging. The sensors are located within a textured surface to accommodate sensor integration into bone. From initial research, surface topography with 30-60 μm features was found to be conducive to guiding new cell growth. Finite element analysis has led to a sensor design for normal and shear stress detection.

I. INTRODUCTION

Clinical management of fractures, bone grafts, and implants relies on x-ray imaging to infer the biomechanical quality of bone regeneration. Recent developments use non-invasive vibratory stimulus to indirectly assess bone stiffness and mass [1]. NASA reported a new device, *Osteosonic^{TM}* [2], to detect the status of damaged tissues and to monitor bone fractures using a sensor that analyzes the vibration response of bone tissue. Nogata et al. 2003 [3], reported estimation of bone strength with ultrasound inspection. Even though some of these methods have good accuracy, they only use the bone density as an indicator of bone strength.

To directly assess the biomechanical properties of bone, extensive work has been done using implanted strain gauges to measure bone strains *in vivo* [4]. While useful as research tools, these sensors are not practical for broad clinical use due to cost, size, ease of use, and power issues. Regarding scale, there are other qualities of bone at a micro-level scale that affect the bone strength, including microarchitecture and damage accumulation [5]. If clinicians had a practical means to directly measure and quantify biomechanical properties of healing or diseased bone *in situ*, within bone, this capability could provide improved and timely information for treatment management options, including drugs, fixation adjustments, rehabilitation regiments, or pre-emptive surgical intervention.

This paper presents the design for an ultra-miniature wireless sensor that can be permanently implanted within bone to measure biomechanical stresses *in situ* at a micro-level scale. The long term goal is to use this sensor to monitor the strength of regenerating bone (open fractures or grafts) or the interfaces between bone and prosthetic implants in order to help guide clinical management of skeletal trauma and disease.

II. TECHNICAL CONCEPT AND PROCESS DESIGN

The model of the proposed sensor is shown in Figure 1. The sensor and coil antenna is fabricated directly on a CMOS chip, with the surface texture for bone growth created by Deep Reactive Ion Etching (DRIE). Beams span from silicon post to post to interconnect the devices. Posts with piezoresistive elements measure the stress applied to the chip. In contrast to the local nature of the validation in single sensor experiments, an array of piezoresistive elements offers the possibility of global data over an entire surface on the order of 1-9 mm^2. The development of such a MEMS stress sensor array also opens the possibility of imaging microscale stress distributions of materials across a surface.
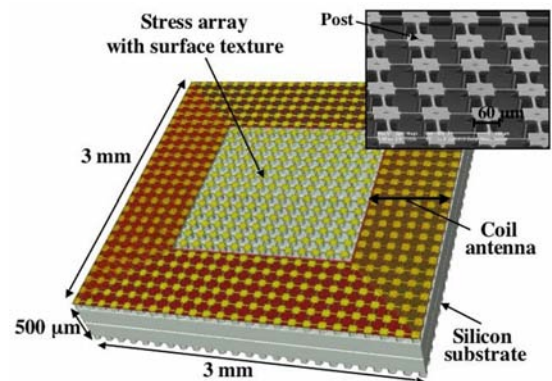

Fig. 1. Integrated implantable bone sensor concept with SEM of the stress sensor prototype. The envisioned final device incorporates a coil antenna on chip. The inset is a prototype of 24 pixels.

A. Surface texturing

Microfabrication has enabled surface features with periodicity, depth, and shape to be precisely controlled. In *in*

vivo results from Chehroudi et al. [6] mineralized tissue was found more frequently on micromachined grooved or pitted surfaces. Guided by this prior work, our group explored several test surface topographic characteristics using microfabrication techniques in silicon prototype chips with a titanium coating. Three basic types of surfaces were chosen: dimple, pimple and pimple/dimple. The texturing exploited the aspect ratio depth etching in the DRIE process (narrow openings in the layout have lower etch rate than wider openings). Figure 2 depicts the textures chosen with simple layouts consisting of an array of square frames with different spacing. Three depths of the topography, 15 μm, 37.5 μm and 60 μm, were created for each texture type.
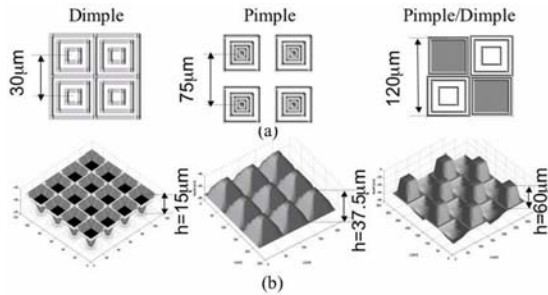

Fig. 2. (a) Layout for pimple, dimple and pimple/dimple textures. (b) 3D surface topography generated with MATLAB.

B. Microfabrication techniques

The chips were processed using DRIE. This is a dry silicon etching technique which involves the use of SF_6/O_2 in a low-pressure inductively coupled plasma (ICP) [7], [8]. A known characteristic of DRIE is its dependence of the etch rates on the aspect ratio of the trench, known as lag or aspect ratio-dependent etching (ARDE). Surfaces can be textured by exploiting ARDE to obtain different levels of heights in an array of microholes of different diameters with the use of one mask [9].

The process starts with a photolithography step that transfers the pattern to a top silicon oxide mask layer for the texturing in a 4"<100> Si wafer that is 400 μm thick. The first DRIE step is a timed etch 340 μm deep to define through holes for additional *in vivo* bone integration. The hole etch was masked with a second photolithography step over the oxide mask layer. After stripping the photoresist, a second timed etch defines the desired surface texture. The intended depth for the texturing is 60 μm at most. The last steps is an isotropic etch, to remove the 2 μm silicon walls left after the prior texturing step. An SEM of a pimple/dimple chip after processing is shown in Figure 3. The entire process flow has been repeated successfully.

C. Cell growth experiments

After the first generation of prototype chips were fabricated, samples were sputter-coated with a thin layer of titanium to provide bio-compatibility for *in vitro* experiments.
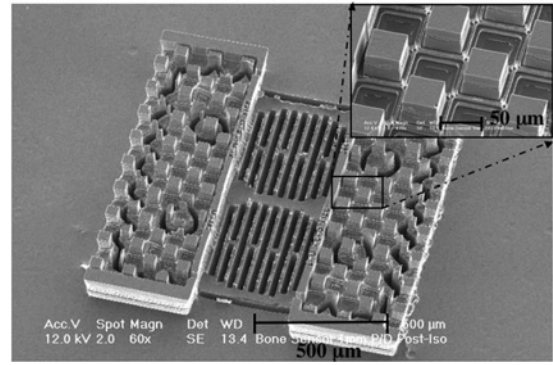

Fig. 3. Prototype chip SEM and detail of 60 μm pimple/dimple texture on the left and right sides of the chip. The central slotted area was texturing for an early design.

The textured surfaces were compared to control groups (non-textured surfaces) to confirm the existance of cell growth on the chips [10]. Cellular attachment was assessed using human Adult Mesenchymal Stem Cells (hAMSC), a cell population isolated from bone marrow that possess the ability to differentiate into multiple cell lineages including osteoblasts. MG-63 cells, a human osteoblast-like cell line, were also used for *in vitro* assessment of cellular interactions with the prototype sensors. Initial studies show that hAMSC and MG-63 cells readily attach, proliferate and remain viable on the surface with all textures. Cell attachment is assessed using live/dead fluorescent staining and scanning electron microscopy (Figure 4). This study has shown high directionality on groove topographies. Further studies after 14 days in a medium containing an osteogenic supplement induced the differentiation of hAMSC into osteoblasts, and resulted in calcium deposition on the prototype sensor.
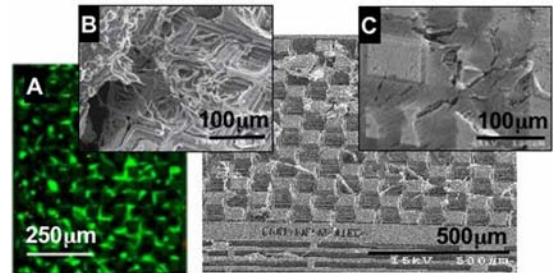

Fig. 4. A. Live/dead fluorescent staining. Green=alive, red=dead. B. SEM characterization of Si sensor with MG-63 cells. C. Si sensor topography underneath layer of hAMSC. [10]

III. STRESS SENSOR DESIGN

This section summarizes the results from a set of ANSYS simulations to verify the mechanics of the sensor inside the bone environment.

A. Finite Element Analysis

A reduced model of the sensor array consists of a silicon substrate, two silicon pillars and a silicon dioxide beam,

enclosed in a cubic cortical bone (Figure 5). The material properties are summarized in Table I. The bone is subjected to a set of axial or shear loads, i.e. a compressive stress applied to opposite sides of the bone.

Material	Young Modulus, E [GPa]	Poisson ratio, ν	Density, ρ, [kg/m^3]
Cortical Bone	18	0.39	2000
Silicon	169	0.3	2330
Oxide	60	0.17	2200

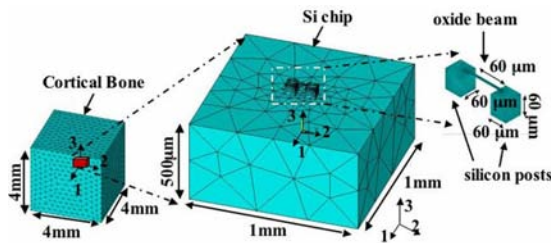[1]The materials are modeled as isotropic.

Fig. 5. ANSYS - simple meshed model of the bone stress sensor.

The two silicon pillars represent part of the texturing that covers the entire surface of the chip. The beam is fabricated as part of the CMOS interconnect stack. It is modelled as oxide although it also contains aluminum wiring. The piezoresistive elements should be placed according to the maximum sensitivity. For the first simulation, a compressive load of 10 kPa is applied to opposite panels of the bone, normal to the *1* axis. Appropriate boundary conditions are set at key points in the remaining panels of the cube. Similar simulations were performed applying a compressive stress along the *2* and *3* axis, and shear stresses (τ_4, τ_5, τ_6) on the side panels of the bone.

Figure 6 shows the stress components across the bone, posts and beam due to a 10 kPa compressive stress. The σ_1 component shows a higher stress with two peaks at the surface of the posts (-8 kPa), but a lower value at the beam (-4 kPa). This provides insight of how the piezoresistive elements should be placed on the posts and not at the beams, to achieve a higher sensitivity during the measurements.

B. Piezoresistive Stress Detection

Piezoresistive silicon is designed through layout of doped resistor areas. The piezoresistance change for a two terminal piezoresistor can be expressed as (1):

$$\frac{\Delta R}{R} = \pi'_{11}\sigma_1 + \pi'_{12}\sigma_2 + \pi'_{13}\sigma_3 + \pi'_{14}\tau_4 + \pi'_{15}\tau_5 + \pi'_{16}\tau_6 \quad (1)$$

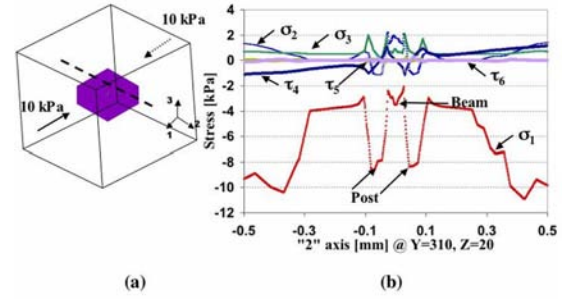where π'_{ij} are the piezoresistive coefficients.

Fig. 6. (a) Sample data line for chip enclosed in cortical bone. (b) Stress components along sample line due to 10 kPa compressive stress.

Dependent on the selection of the piezoresistor arrangement relative to crystal orientation, the sensitivity is maximized. FEA provides the compressive or shear stress values to calculate (1). The two sets of piezoresistive arrangements in Figure 7 were studied. Selecting the [100] direction for *n*-type piezoresistors and [110] for *p*-type, gives the maximum sensitivity according to FEA results. For piezoresistors oriented in the [100] it is necessary to use a coordinate transformation to find the corresponding stress components with respect to the primed coordinate frame (*1',2',3'*).
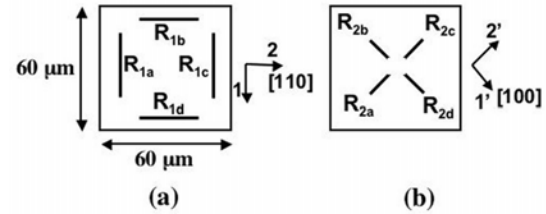

Fig. 7. (a) Piezoresistors oriented in the [110] direction. (b) Piezoresistors oriented in the [100] direction.

The resistance change for piezoresistors in [110] orientation (Figure 7(a)) is:

$$\frac{\Delta R_1}{R_1} = \frac{1}{2}(\pi_{11} + \pi_{12} + \pi_{44})\sigma_1 + \frac{1}{2}(\pi_{11} + \pi_{12} - \pi_{44})\sigma_2 + \pi_{12}\sigma_3 \quad (2)$$

and in [100] orientation (Figure 7(b)) is:

$$\frac{\Delta R_2}{R_2} = \left(\frac{\pi_{11} + \pi_{12}}{2}\right)\sigma_1 + \left(\frac{\pi_{11} + \pi_{12}}{2}\right)\sigma_2 + (\pi_{11} - \pi_{12})\sigma_3 + \pi_{12}\sigma_3 \quad (3)$$

C. Stress Tensor Derivation

A Wheatstone bridge configuration is selected to measure the change in resistance in order to cancel common mode influences, primarily temperature. From the structural analysis in section III.A, it is possible to design piezoresistance elements within a bridge to isolate a single component of

the stress sensor. Since the entire chip consists of an array of posts, the bridge circuits can be distributed to maximize the fill factor in one cell. The change of piezoresistance given an input load (compressive or shear) for all *n*-type and *p*-type element combinations was calculated through simulations. For a post with *p*-type piezoresistors oriented in the [110] direction (Figure 7(a)) the output voltage is:

$$V_{o1} = \frac{1}{4} \left[\frac{\Delta R_{1b} + \Delta R_{1d}}{R_{1b} + R_{1d}} - \frac{\Delta R_{1a} + \Delta R_{1c}}{R_{1a} + R_{1c}} \right] V_s \qquad (4)$$

Table II shows the output voltage for different bridge circuits. In bridges 4, 5, 6 the compressive loads applied to the bone model do not have any effect on the output. On the other hand, the shear loads will produce an output shift.

TABLE II

ΔV FOR BRIDGES DUE TO EXTERNAL LOAD APPLIED.

	ΔV_1	ΔV_2	ΔV_3	ΔV_4	ΔV_5	ΔV_6
dir.	[110]	[110]	[100]	[110]	[110]	[100]
doping	*p*-type	*p/n*-type	*p*-type	*p*-type	*p*-type	*n*-type
σ_1	-	0	0	0	0	0
σ_2	+	+	0	0	0	0
σ_3	0	-	+	0	0	0
τ_4	0	0	0	-	0	0
τ_5	0	0	0	0	+	0
τ_6	0	0	0	0	0	-

The output voltage from each piezoresistive bridge needs to be amplified, and care must be taken to design the amplifier with sufficiently low thermal and flicker noise. For a minimum stress of 100Pa, and using the longitudinal piezoresistive coefficient, the output voltage is 0.359mV. The calculated thermal noise is 1.92nV/rtHz for a single 10 μm x 0.35 μm piezoresistor, at room temperature and a 1Hz bandwidth. Adding a typical noise for a simple amplifier the signal to noise ratio (SNR) is 34.1 dB.

IV. RESULTS

A chip with a 6x6 array and electronics has been processed through the Jazz SiGe 0.35μm BiCMOS process. Figure 8 shows an SEM after a 60 μm DRIE and a short isotropic etch to release the beams. Four diffused piezoresistors were placed on each post as was described in Figure 7. Six combinations of *n*-type and *p*-type bridges are used to extract the six stress components. The bondpads are used to electrically characterize each post before and after release, as well as for future mechanical characterization. The measured resistances for an *n*-type bridge were: R_{1a}=3.1kΩ, R_{1b}=2.8kΩ, R_{1c}=3.2kΩ, and R_{1d}=3.0kΩ. A mechanical set-up is under construction to evaluate the performance of the sensor in a material with similar mechanical properties as the bone.
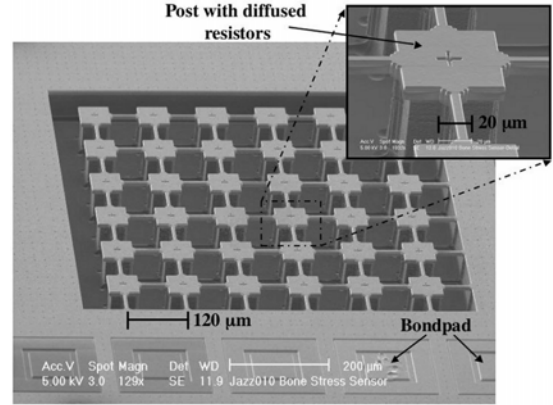

Fig. 8. SEM of chip with 6x6 array after DRIE and isotropic etch. The inset shows a post with diffused piezoresistors on the Si below the metal/oxide.

V. CONCLUSION

This paper presents a new approach to directly measure bone stress *in situ* at a micro-level scale through an implantable MEMS stress sensor. The array of piezoresistive elements provides the capability to extract the stress tensor in a material with statistical analysis of stress. A model of the sensor is developed and will be verified. This instrument may be used to validate bone stress data from FEA models at a micro-level scale, where the analysis is complex and separate phenomena occur, such as crack, friction or decohesion.

REFERENCES

[1] J. Haggerty (1996) "Mechanical Response Tissue Analyzer," Spinoff 1996, NASA, Office of Space and Technology, [Online]. Available: http://www.sti.nasa.gov/tto/spinoff1996/24.html
[2] M. Liebshner, "OsteoSonic^{TM}, Noninvasive bone and joint damage detection device," NASA Tech Briefs, April 2004.
[3] F. Nogata, A. Shimamoto and T. Habu "Estimation of in-vivo bone strength using ultrasound signals," *International Journal of Modern Physics B*, vol. 17, nos. 8 & 9, pp. 1381-1387, 2003.
[4] Hoshaw, et al., "A method suitable for in vivo measurement of bone strain in humans," *Journal of Biomechanics*, Vol. 30, No. 5, pp. 521-524, 1997.
[5] J. Bilezikian, et al., "Osteoporosis: Diagnosis, treatment, and monitoring considerations," 3rd ed. *Continuing Medical Education Forum*, vol 3., no. 1, March 2004.
[6] B. Chehroudi, D. McDonnel, and D.M. Brunette, "The effects of micromachined surfaces on formation of bone-like tissue on subcutaneous implants as assessed by radiography and computer processing," *J. Biomedical Materials Res.*, vol. 34, pp. 279-290, 1997.
[7] X. Zhu, "PostCMOS Micromachining of Surface and Bulk Structures," PhD Thesis, CMU, May 2000.
[8] F. Larmer and P.Schilp, "Method of anisotropically etching silicon," German Patent DE 4241045, 1994.
[9] T. Bourouina, T. Masuzawa and H. Fujita, "The MEMSNAS Process: Microloading Effect for Micromachining 3-D Structures of Nearly All Shapes," *Journal of Microelectromechanical Systems*, vol. 13, no. 2, pp. 190-199, 2004.
[10] C. Heyward, "The importance of CMOS surface topography in the attachment, proliferation, and differentiation of human adult mesenchymal stem cells," Masters Thesis, Duquesne University, July 2004.